Lateral Reorganization of Fluid Lipid Membranes in Response to the Electric Field Produced by a Buried Charge

Jay T. Groves,[†] Steven G. Boxer,* and Harden M. McConnell

Department of Chemistry, Stanford University, Stanford, California 94305-5080

Received: June 30, 2000; In Final Form: September 26, 2000

A thermodynamic model describing multicomponent fluid membranes under the influence of lateral forces due to a buried charge is developed to estimate the magnitude and dynamics of field-induced lateral reorganization in membranes of living cells. The calculations were performed for an electric field geometry such as might be produced by a charge in an ion channel but can apply to any situation where charge is buried in the low dielectric environment of a membrane, for example, during electron transfer. The model includes molecular size and charge differences as well as critical demixing effects. These calculations indicate that the local concentration of charged and uncharged membrane components can be substantially altered over the course of a few microseconds. Critical demixing effects enhance the propensity of a membrane toward lateral reorganization and provide an intriguing mechanism by which an electric field can induce separation between neutral molecules such as cholesterol and phosphatidylcholine.

Introduction

Cell membranes are generally fluid structures with their molecular components exhibiting rapid diffusion in the plane of the membrane. This fluid-mosaic system is able to undergo lateral reorganization in response to factors such as bending,[1−5] sheer,[6] adhesion,[7,8] or electric fields.[9] The magnitude and extent of such reorganization depends on a balance between the relevant forces and the effects of entropy.[10−12] Lateral organization of membranes plays an important role in numerous cellular processes.[13−18] Additionally, the manner in which proteins and other membrane components perturb the local lipid distribution can affect larger scale organizational tendencies such as clustering and compartimentalization.[19−23]

In this paper, a continuum thermodynamic model is employed to estimate the dynamic lateral reorganization of fluid membranes in response to naturally occurring electric fields. There already exists an extensive body of work concerning the effects of transmembrane electric fields. Here, we focus primarily on *lateral* fields and their ability to move molecules in the plane of a lipid bilayer. The response of a fluid membrane to the field produced by a single charge in the membrane plane is calculated under physiological conditions. This configuration is chosen as a plausible model for the type of field geometry that is produced when a charge passes through a cell membrane. It applies generally to a variety of situations involving charges forced into interior regions of a lipid bilayer, for example, by electron transfer or a conformational change of a protein.

In these calculations, the membrane is treated as a quasi three-component system consisting of cholesterol, neutral lipids, and negatively charged lipids. This composition resembles that of the red blood cell membrane. The calculations reveal lateral membrane reorganization, several nanometers in extent, occurring on the microsecond time scale. Two distinctively different attributes of the reorganization are investigated. The most direct response of a fluid membrane mixture to lateral electric fields is electrostatic reorganization. The density of charged membrane lipids can be enriched by more than a factor of 3 or nearly completely depleted depending on the direction of the field for the force profiles examined here. The corresponding changes in local membrane surface potential can be more than 40 mV. This suggests a mechanism by which the membrane can influence the local electrostatic environment of an ion channel in response to the passage of charges.

The role of critical demixing effects in the membrane reorganization is also examined. Critical demixing is a collective molecular interaction which gives rise to spontaneous phase separation at appropriate temperatures and compositions. It introduces an additional thermodynamic force which has the effect of amplifying the lateral reorganization of fluid membranes in response to external forces. This has been observed experimentally in supported lipid membranes[24] and in lipid monolayers at the air−water interface.[25] Furthermore, there is experimental evidence suggesting that lipid extracts from red blood cell membranes are near a miscibility critical point between cholesterol and the phospholipid components.[26] In the calculations described below, it is found that critical demixing effects enable an electric field to induce separation between neutral molecules. This quasi electric field-induced phase separation may have implications for the role played by cholesterol in cell membrane organization. It also suggests an electrostatic mechanism by which proteins could preferentially associate with cholesterol-rich membrane domains.

Thermodynamic Model

The time-dependent reorganization of a membrane in response to lateral forces is computed from the set of chemical potentials $\{\mu_k\}$ as follows:

$$\frac{\partial \varphi_k}{\partial t} = \eta_k \nabla\cdot(\varphi_k \nabla \mu_k) \tag{1}$$

The area fraction of component k is φ_k and the corresponding electrophoretic mobility is η_k. Typical mobility coefficients for

* Address questions to this author: Sboxer@Stanford.edu; 650-723-4482.
[†] Current address: Lawrence Berkeley National Laboratory, 1 Cyclotron Road Bldg. 3, Berkeley, CA 94720.

10.1021/jp002320a CCC: $19.00 © 2000 American Chemical Society
Published on Web 10/28/2000

double chain phospholipid molecules in bilayer membranes are around 1.1×10^{21} $\mu m^2/(J\ s)$;[27−29] this value was used for the phospholipid components in the calculations below. Cholesterol was assumed to have an average molecular area in the membrane of 35 Å^2, while that of the phospholipids was taken to be 60 Å^2.[29−31] Within a given membrane, the mobility of molecules scales inversely with their effective molecular area; thus the mobility coefficient of cholesterol is 1.7 times the value mentioned above. (For a more thorough discussion of the relation between two-dimensional mobility and molecular area in multicomponent membranes see ref 32.) The gradients of the chemical potentials used here are given by

$$\nabla\mu_k = k_B T\left(\frac{1}{\varphi_k}\frac{\partial\varphi_k}{\partial r} + \sum_i\left(\frac{A_{mi} - A_{mk}}{A_{mi}}\right)\frac{\partial\varphi_i}{\partial r}\right) + \frac{A_{mk}}{A_u}\sum_{i,j}\gamma_{ij}(\delta_k^i - \varphi_i)\frac{\partial\varphi_j}{\partial r} + A_{mk}\frac{\partial\Pi}{\partial r} - A_{mk}f_k + z_{mk}e\frac{\partial\psi}{\partial r} \quad (2)$$

where k_B is the Boltzmann constant, T is the temperature, r is the radial position, A_u is the unit area of the lattice (equal to the smallest of the molecular areas), and δ_k^i represents the Kronecker delta function defined as $\delta_k^i = \{1$ for $i = k$; 0 for $i \neq k\}$. In this representation, membrane components are characterized by their effective molecular areas (A_{mk}), molecular charges ($z_{mk}e$), and the set of critical demixing coefficients (differential interaction energies) between each of the different species present $\{\gamma_{ij}\}$. Each element, γ_{ij}, is directly related to the critical temperature in the corresponding binary mixture, thus offering a link between measurable parameters in simplified systems and the behavior of complex mixtures. The long-range lateral forces acting on each component are represented by f_k in terms of force per unit area. Short-range electrostatic interactions such as those among the charged lipids in the membrane are computed using a continuum electrostatic model (Gouy−Chapman theory) to determine the local surface potential, ψ, from the membrane composition. The two leaflets of the bilayer membrane are treated independently since, at physiological ionic strength, they are electrostatically isolated from each other.[33] In this case, the surface charge density, σ, is given by

$$\sigma = \sum_i \frac{z_{mi}e}{A_{mi}}\varphi_i \quad (3)$$

and is related to the surface potential by the Gouy equation:

$$\psi(\sigma) = \left(\frac{2k_B T}{ze}\right)\sinh^{-1}\left(\frac{\sigma z e L_D}{2k_B T\epsilon_w}\right) \quad (4)$$

where z is the valence of the symmetrical electrolyte solution, e is the elementary charge, ϵ_w is the dielectric constant of water, and L_D is the Debye length defined as $L_D = (k_B T\epsilon_w/2Iz^2e^2)^{1/2}$ with I denoting the ionic strength of the bulk solution.

This thermodynamic model specifically describes fluid mixtures which, in the absence of applied lateral forces, consist of a single thermodynamic phase. However, it is applicable to intrinsically multiphase systems as long as the individual phase domains are treated separately. This model has been used to describe experimental electric field-induced concentration profiles in supported membranes and is discussed in detail elsewhere.[12,24,32]

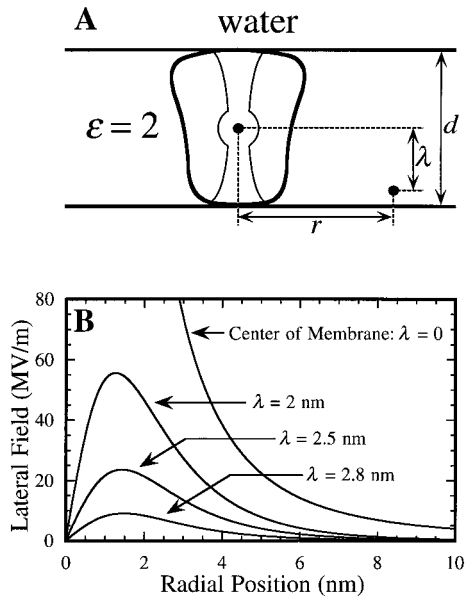

Figure 1. (A) Diagram illustrating the electric field geometry and coordinate system used in the cell membrane calculations described here. The membrane is treated as a slab of dielectric material embedded in a conducting medium. The membrane thickness is d, λ refers to the distance from the center of the membrane of the charge on the lipid, and r is the radial distance from the source charge positioned in the middle of the membrane. (B) Plots of the parallel component of the electric field, $E_{||}$, as a function of radial position, r, at different vertical depths, λ, in the membrane. The $\lambda = 2.5$ nm value was assumed to correspond most closely to the situation of a net charge located in the lipid headgroup.

Cell Membranes

Electric Fields. To better understand the physical nature of membranes in living cells, we use the thermodynamic model outlined above to calculate the magnitude and rate of lateral membrane reorganization that could occur under physiological conditions. Long-range electric fields can propagate laterally along the low-dielectric core of lipid membranes despite the fact that the Debye length within aqueous compartments of a cell is less than 1 nm. In particular, the field due to a single charge in the membrane, such as an ion passing through an ion channel, is examined. We stress at the outset that the model developed here is meant to provide an estimate for the type, mangitude and time scale of effects which might be observed, not a detailed molecular-scale calculation for any particular system.

An estimate of the electric field produced by a charge in a membrane can be made by treating the membrane as a slab of dielectric material embedded in a conducting medium (Figure 1). Lipid membranes are generally ascribed an effective dielectric constant of $\epsilon = 2$, which is similar to that of a protein interior ($\epsilon = 2-4$).[34,35] In these calculations the protein and membrane regions are treated as a single dielectric medium with an average dielectric constant of $\epsilon = 2$. Of course, actual phospholipid bilayers present a more complicated dielectric medium which is not homogeneous. However, for the present purposes, a rough estimate of conceivable field geometries and magnitudes is sufficient. The immediate environment of the embedded ion is expected to be highly polarizable in order to reduce the formidable amount of energy required to move a charge into the low-dielectric membrane core. For example, the X-ray crystal structure of the potassium channel reveals a 10 Å diameter water-filled cavity in the center of the channel which contains a potassium ion.[36] The water screens the ion, effectively

distributing the charge over a larger volume. Although this substantially reduces the electrostatic energy, it follows from Gauss' law that the total electrical flux through an enclosing surface outside the solvation region is unchanged. Thus, long-range electric fields in the membrane are not necessarily influenced significantly by local screening effects.

The electric field components for the geometry illustrated in Figure 1A are easily computed by the method of image charges:

$$E_{||} = \frac{1}{4\pi\epsilon_m} \sum_{i=-\infty}^{\infty} \frac{ze(-1)^i r}{(r^2 + (\lambda + id)^2)^{3/2}} \quad (5)$$

$$E_{\perp} = \frac{1}{4\pi\epsilon_m} \sum_{i=-\infty}^{\infty} \frac{ze(-1)^i (\lambda + id)}{(r^2 + (\lambda + id)^2)^{3/2}} \quad (6)$$

where ϵ_m is the dielectric constant of the membrane, r represents the radial distance from the source charge, λ is the distance from the midplane of the membrane, and d is the total thickness of the membrane. Several plots of $E_{||}$ for different values of λ are illustrated in Figure 1B. The membrane thickness, d, was taken to be 6 nm in these calculations. This value was chosen to be slightly larger than a typical membrane thickness of 5 nm to account for the Gouy−Chapman double layer. The Debye length at physiological ionic strength (150 mM) is about 8 Å, thus counterions in the water are, on average, several angstroms away from the membrane. When treating the water as a conductor, its edge is defined by the location of these counterions.

The parallel component of the electric field, $E_{||}$, acts on the membrane in much the same way as the externally applied tangential fields, which have been studied experimentally. For calculations of the long-range electrostatic force profile, charges on lipids in the membrane are assumed to be located in a plane 2.5 nm away from the midplane of the bilayer ($\lambda = 2.5$ nm). This corresponds to a charge located in the lipid headgroup. The notation $f(r)$ will be used to represent the magnitude of the force profile obtained from these parameters; a superscript + or − specifies the sign of the central charge. For purposes of comparison, a range of different force profiles is also considered. The long-range electrostatic force is analogous to the electrophoretic force in the case of the supported membrane experiments.[12,24] Short-range electrostatic interactions such as those between charged lipids in the membrane are treated separately using Gouy−Chapman theory. In this way, the nonlinear interaction between overlapping clouds of counterions in the diffuse layer is included in the model.

Membrane Reorganization. The field-induced reorganization in three-component membranes resembling the inner leaflet of a red blood cell membrane was calculated according to eq 1. The model membranes were composed of cholesterol (CH), negatively charged phosphatidylserine (PS), and neutral lipids such as phosphatidylcholine (PC) with average area fractions of 0.33, 0.12, 0.55, respectively. Although the membrane components mentioned above are intended to model cholesterol, PS, and PC, no explicit distinction is made regarding detailed chemical composition in the thermodynamic model. Each fraction represents a generic collection of membrane components categorized by charge, average molecular area, and the demixing characteristics described below.

Concentration gradients present at 1, 10, and 100 μs after the appearance of the field from a positive or negative central charge are plotted in the six panels of Figure 2. These calculations are two-dimensional solutions generated from eq 1 in polar geometry; they depict radial distributions of the membrane components around a central charge. The solid curves represent concentration profiles expected when critical temperatures for binary mixtures of CH/PS, T_c^{12}, and CH/PC, T_c^{13}, are both taken to be 2 K below the ambient temperature of 295 K ($T_c^{12} = T_c^{13} = 293$ K). The PC and PS are assumed to mix ideally implying a binary critical temperature, T_c^{23}, of 0 K (we use the numbering scheme: CH = 1, PS = 2, PC = 3). Although the precise values of these critical temperatures are not known, there is experimental evidence indicating that lipid extracts from red blood cell membranes with compositions resembling the one used in these calculations are near a miscibility critical point between cholesterol and the phospholipid components at room temperature.[26] There is also evidence from supported membrane experiments suggesting that egg-PC and PS mixtures exhibit nearly ideal mixing.[12] The binary critical demixing coefficients corresponding to this situation are: $\gamma_{12} = 2.65\ k_B T_c^{12}$, $\gamma_{13} = 1.55\ k_B T_c^{13}$, and $\gamma_{23} = 3.68\ k_B T_c^{23} = 0$. The relation between critical demixing coefficients and critical temperatures in multicomponent membranes depends on the effective molecular areas and charges as well as the electrostatic environment of the membrane.[24,32] For comparison, calculated profiles assuming ideal mixing between all three components are plotted with dashed curves in Figure 2.

Details of the electrostatic interaction between an ion located in the membrane interior and charged membrane lipids are complex. For example, hydration shell waters around the polar lipid headgroups will raise the average dielectric constant within this region. This will decrease the electric field experienced directly at the position of the charged moiety on a membrane lipid. However, the influence of this type of solvation on the net force transmitted to a charged lipid is less clear. In the process of screening electric fields, hydration shell waters and other polarizable groups will necessarily experience forces themselves; these forces will be mechanically transmitted to other molecules with which they are interacting. The force profiles used to calculate the membrane reorganization depicted in Figure 2 are strictly Coulombic forces resulting from the electric field geometry illustrated in Figure 1. To explore the consequences of screening and other mitigating factors, calculations for a range of different force profiles are also examined to characterize the force dependence of the membrane response. Concentration profiles of cholesterol induced by four linear scalings (1×, 0.5×, 0.2×, and 0.1×) of the force profile examined in Figure 2, $f^-(r)$, with $T_c = 293$ K are plotted in Figure 3A. A significant observation from these calculations is that the membrane response shows a highly nonlinear dependence on force. Although the time scale of reorganization varies, there is a nearly binary outcome whereby a quasi phase separation is induced if threshold conditions are met. For the membrane composition examined here, an average lateral force of 0.5×10^{-12} N/molecule on the charged lipid extending for 2 nm is about the threshold for induction of the quasi phase separation. This is one-fifth of the Coulombic force profile used for the calculations in Figure 2. We note that biological situations involving larger forces may exist, for example where multiple charges are involved, but we focus on reduced force profiles because the calculated membrane reorganization is already substantial.

The most influential factor affecting field-induced reorganization in lipid membranes is critical demixing. This substantially enhances the magnitude of the reorganization as can be seen clearly in the profiles plotted in Figures 2 and 3B. Particularly large effects are found in calculations of reorganization induced

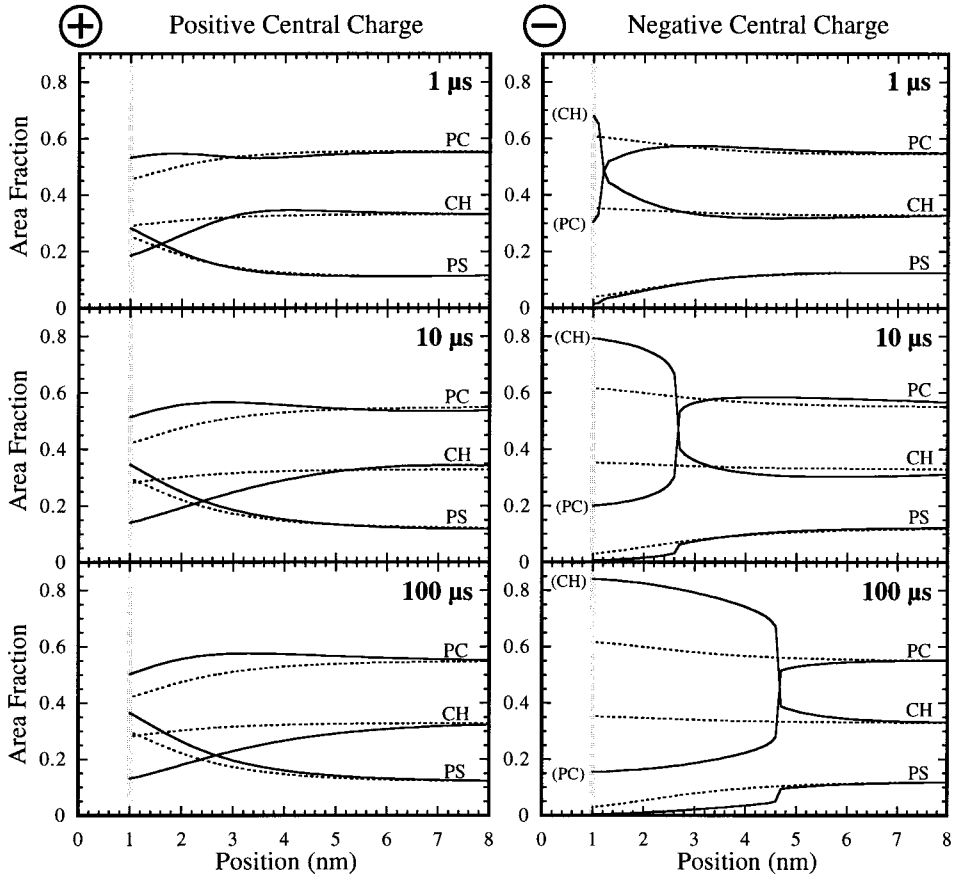

Figure 2. Calculations of the membrane reorganization caused by interaction of the parallel electric field from the geometry illustrated in Figure 1A with charged lipids in the membrane. These curves represent two-dimensional solutions generated from eq 1 in polar geometry; they depict radial distributions of the membrane components around a central ion. Charges on the membrane lipids are assumed to be in a plane 2.5 nm away from the midplane of the bilayer ($\lambda = 2.5$ nm) which corresponds to a charge in the lipid headgroup. The vertical gray bar indicates the boundary of the hypothetical ion channel. A three-component membrane consisting of cholesterol (CH), PS, and PC at average area fractions of 0.33, 0.12, and 0.55 respectively is modeled in these calculations. The cholesterol was taken to have an average molecular area in the membrane of 35 Å^2 while the PS and PC were each assumed to occupy 60 Å^2 per molecule. Concentration gradients present at 1, 10, and 100 μs after the appearance of the field are shown for both positive and negative central charges at an ambient temperature of 295 K. The dashed curves were calculated allowing ideal mixing among all three components. The solid curves depict calculated profiles when the system is roughly 2 K above the miscibility critical temperature between cholesterol and the phospholipid components ($T_c^{12} = T_c^{13} = 293$ K). The critical demixing coefficients representing this situation are $\gamma_{12} = 2.65k_BT_c^{12}$, $\gamma_{13} = 1.55k_BT_c^{13}$, and $\gamma_{23} = 0$ (for discussions of the relationship between critical demixing coefficients and critical temperatures in membranes see refs 24 and 32).

by a negative central charge. The asymmetric response with respect to the direction of the field is related to the fact that the sensitivity of the membrane to lateral perturbations depends strongly on membrane composition. Under the influence of a negative central charge, the local composition of the membrane shifts toward compositions which are more sensitive to the electric field. This process is diagrammed in Figure 4. As the membrane composition changes from the initial composition (Φ_i) to the final local composition around a negative central charge (Φ_f^-), it approaches and crosses a line of critical compositions. At temperatures above the highest critical temperature, the greatest sensitivity toward lateral perturbations occurs at the critical compositions.[32] In the case of the positive central charge, the composition shifts to a less sensitive region of the phase space (point Φ_f^+ in Figure 4). The polarity of this effect depends on the initial composition; membranes with different compositions could exhibit increased sensitivity toward reorganization induced by a positive central charge.

The composition dependence of membrane sensitivity is of particular interest in light of emerging evidence for direct cluster formation between cholesterol and certain phospholipids.[37,38] One consequence of such clustering is to alter the effective size of the cholesterol-containing objects in the membrane. This changes the effective composition of the membrane as well as shifting the critical compositions. Moderate clustering of cholesterol with phospholipid components in a mixture with the composition studied here could shift the system closer to a critical composition.

Demixing effects also substantially affect the time scale of reorganization. This phenomenon is known as critical slowing down, referring to the markedly decreased rate at which a system near a critical point approaches its equilibrium configuration. Though present in both cases, critical slowing down is most apparent in calculations of profiles induced by the negative central charge. When all three components are taken to mix ideally, the system essentially reaches its equilibrium distribution in less than 10 μs. In contrast, when the lipid mixture is near a critical or spinodal point, the reorganization process proceeds roughly 2 orders of magnitude more slowly.

In addition to increasing the magnitude and time scale of the membrane reorganization, critical demixing effects provide a mechanism by which neutral components such as cholesterol and PC can be separated by an electric field. Note the significant enrichment of cholesterol and concomitant depletion of PC around the negative source charge when the membrane is near a critical point. The reverse effect is observed, to a lesser extent,

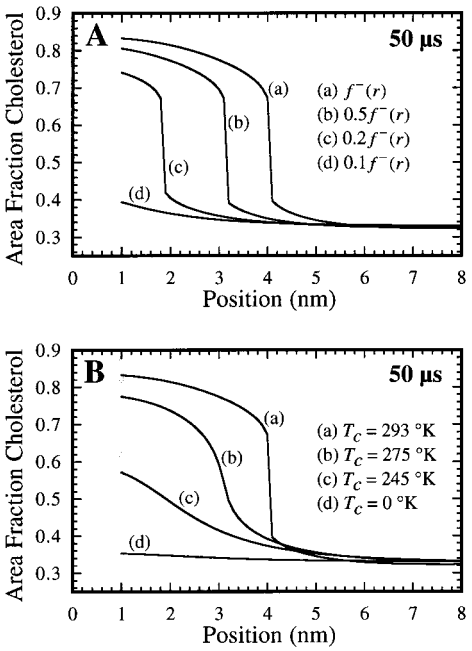

Figure 3. (A) Comparison of cholesterol concentration profiles after 50 μs induced by several linear scalings of the $f^-(r)$ force profile used in Figure 2. $T_c = 293$ K for these calculations; all other parameters in both A and B are identical to those used in Figure 2. (B) Plots of cholesterol concentration profiles induced by the $f^-(r)$ force profile after 50 μs assuming different degrees of critical demixing. The four concentration profiles were calculated for systems differing only in the value of the binary critical temperatures assigned to CH/PS and CH/PC mixtures (as labeled).

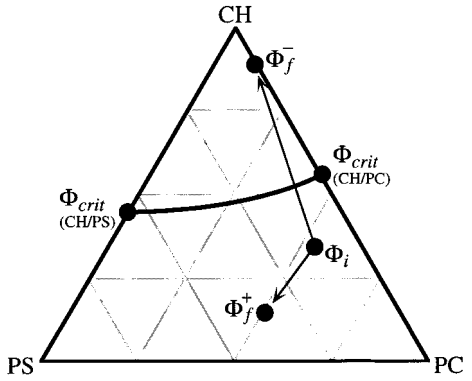

Figure 4. Schematic of the ternary composition phase space for a CH/PS/PC membrane in terms of area fraction. The ternary composition, Φ, is defined as (φ_{CH}, φ_{PS}, φ_{PC}). Critical compositions for binary mixtures of CH/PS, $\Phi_{crit} = (0.44, 0.56, 0)$, and CH/PC, $\Phi_{crit} = (0.57, 0, 0.43)$, are labeled with points while a solid curve traces the locus of critical compositions in the ternary mixture. Each critical composition is associated with a critical temperature giving rise to a continuous set of critical points in the temperature−composition phase space. Point Φ_i marks the initial composition of the membranes considered here, (0.33, 0.12, 0.55). Points Φ_f^- and Φ_f^+ mark the compositions at the 1 nm position (see Figure 2) after 100 μs of reorganization due to negative and positive central charges, respectively.

with the positive source charge (Figure 2). This separation results from a pressure gradient that is induced by direct action of the parallel electric field on the charged PS lipids. The field-induced pressure gradient, in turn, imparts a force on all components in the membrane. Critical demixing effects break the symmetry between cholesterol and PC thus providing a means to separate these uncharged components. As an interesting corollary, this suggests an electrostatic mechanism by which proteins could preferentially associate with cholesterol-rich domains in the membrane. A related phenomenon has been observed experimentally in cardiolipin/egg-PC/NBD-PE membranes.[24] Cardiolipin and NBD-PE have roughly the same charge per area thus they, like neutral molecules, cannot be separated solely by the action of a tangential electric field. The nonmonotonic concentration profile of the NBD-PE probe lipid seen in supported membrane experiments corresponds to a field-induced separation of NBD-PE from cardiolipin and is a direct manifestation of this type of critical demixing effect.

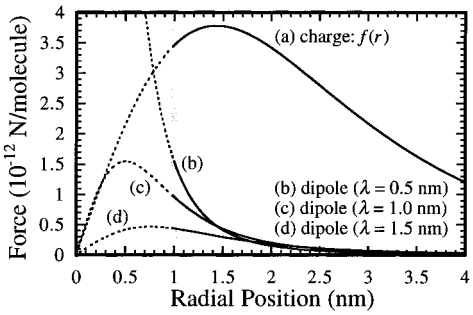

Figure 5. Comparison of the force profile, $f(r)$, resulting from the direct Coulombic interaction of a net charge with $E_{||}$ (a) and the force profiles on molecular dipoles due to the field gradient. (b)−(d) illustrate this dipolar force profile for a perpendicular dipole moment of 0.75 D at different depths in the membrane. Forces at radial positions within one nanometer of the central source charge are drawn with dashed lines to indicate that, in most situations, fluid membrane is not expected to reach within this region.

Dipole Effects. The electric field geometry illustrated in Figure 1 will also impart a net lateral force on neutral molecules if they have a dipole moment oriented perpendicular to the membrane plane. This arises from the fact that $E_{||}$ is a function of vertical position (λ) within the membrane. A neutral molecule with partial charges at different vertical positions will experience a net force since $E_{||}$ is different for each of the partial charges. The magnitude of this force is given by $M_k\, \partial E_{||}/\partial\lambda$ where M_k is the corresponding molecular dipole moment perpendicular to the membrane plane. This can be expressed more conveniently in terms of $E_\perp$ (eq 6) by making use of Maxwell's equation, $\nabla \times \mathbf{E} = 0$, which implies that $\partial E_\perp/\partial r = \partial E_{||}/\partial\lambda$. Consequently, molecules in the membrane experience a lateral force, F_k, proportional to the product of their perpendicular dipole moment and the lateral gradient of $E_\perp$:

$$F_k = M_k \frac{\partial E_\perp}{\partial r} \tag{7}$$

This inhomogeneous field effect has been observed experimentally in lipid monolayers at the air−water interface using an insulated wire to produce the field gradient.[25] Dramatic field-induced reorganization was seen when the lipid mixture was maintained near a critical point.

In the field geometry examined here, lateral dipolar forces related to the field gradient are weaker and shorter range than those due to interactions between net charges and the parallel field. Curve (a) in Figure 5 is the force profile for the interaction of a single net charge in the lipid headgroup ($\lambda = 2.5$ nm) with the parallel field component. This is the force profile, $f(r)$, used in the calculations depicted in Figure 2. Curves (b)−(d) of Figure 5 illustrate the force profiles experienced by a neutral molecule with a dipole moment of 0.75 D centered at different vertical positions in the membrane. The largest effect is found near, but not at, the midplane of the membrane. The dipolar force goes through a node precisely at the center of the membrane.

TABLE 1: Values of $\Delta\psi_{max}$ (mV)[a]

force	T_c (K)	1 μs	10 μs	100 μs
$f^+(r)$	293	−31.4	−40.4	−42.9
$f^+(r)$	0	−26.8	−33.6	−33.8
$f^-(r)$	293	+28.3	+30.9	+31.5
$f^-(r)$	0	+21.3	+24.0	+24.1
$0.2f^+(r)$	293	−6.7	−9.0	−9.4
$0.2f^+(r)$	0	−5.1	−6.4	−6.4
$0.2f^-(r)$	293	+6.6	+20.8	+23.0
$0.2f^-(r)$	0	+5.0	+6.0	+6.0
$0.1f^+(r)$	293	−3.3	−4.6	−4.8
$0.1f^+(r)$	0	−2.5	−3.0	−3.0
$0.1f^-(r)$	293	+3.3	+5.0	+5.9
$0.1f^-(r)$	0	+2.5	+3.1	+3.1

[a] Computed with the Guoy equation (eq 4) for uniform charge densities corresponding to the maximum or minimum surface charge densities from the concentration profiles. $f^+(r)$ and $f^-(r)$ represent the force profiles for positive and negative central charges used for the calculations in Figure 2. Values of $\Delta\psi_{max}$ induced by 1×, 0.2×, and 0.1× fractional force profiles are tabulated above.

In a real membrane, dipolar forces would be superimposed on the direct field effects serving to slightly modify the reorganization.

Electrostatic Consequences. The field-induced reorganization of charged membrane lipids around an ion channel could feasibly influence ion transport across membranes. There are a number of examples where membrane charge density is known to affect ion transport through channels.[39] As seen in Figure 2, the local charge density in the membrane immediately surrounding an ion channel could be increased by more than a factor of 3 or almost completely depleted due to the electric field from a charge in the channel. For a simple comparison, define $\Delta\psi_{max}$ as the relative change in surface potential between the bulk membrane and the region immediately surrounding the protein resulting from the field induced reorganization. Values of $\Delta\psi_{max}$ corresponding to the concentration profiles plotted in Figure 2 along with concentration profiles generated from scaled force profiles were computed using Gouy−Chapman theory and are listed in Table 1.

Several different types of behavior are evident in the calculations of electrostatic reorganization. For the unscaled force profiles, $f^+(r)$ and $f^-(r)$, corresponding to the concentration profiles illustrated in Figure 2, $\Delta\psi_{max}$ values are large and only mildly influenced by critical demixing effects. Changes in surface potential of this magnitude can alter the potential energy of nearby ions by 2−4 kJ/mol. Critical demixing effects tend to increase the magnitude of $\Delta\psi_{max}$ by 20−30% over the ideal case for the unscaled force profiles. This is a relatively small enhancement compared to the effect of demixing on concentration profiles of cholesterol and PC. At these forces and charge densities, electrostatic repulsion among charged lipids in the membrane is the limiting factor. The apparent field produced by the inhomogeneous distribution of charged membrane components ($\partial\psi/\partial r$) can be on the order of 10 MV/m and opposes reorganization.

The force profiles scaled by 0.2 are close to the threshold for induction of the quasi phase separation discussed earlier (Figure 3). Effects of critical demixing on electrostatic reorganization are substantially more prominent at these lower forces. Note especially the 4-fold increase in $\Delta\psi_{max}$ over the ideal case for the $0.2f^-(r)$ force profile. The 0.1x scaled force profiles are below the threshold for induction of any type of quasi phase separation behavior for this membrane composition. However, demixing effects still significantly increase the magnitude of electrostatic reorganization. Experimentally, critical demixing in the membrane has been demonstrated to have a pronounced effect on ion channel conductivity.[40]

It can be seen from the calculations in Table 1 that the predominant electrostatic reorganization generally occurs within a few microseconds. This is fast compared to the channel gating which typically takes place on the millisecond time scale.[41] Thus, channels which are occupied a majority of the time during ionic conduction are expected to induce a steady-state reorganization of the membrane similar to that of a constant charge. Multiply occupied channels such as the potassium channel are likely to be in this category.

Conclusion

The calculations described above provide an estimate of the type of dynamic and steady-state field-induced reorganization that could occur in cell membranes. A simple model of an ion embedded in a membrane suggests that this electric field can substantially alter the composition of the surrounding fluid membrane. The time scale of reorganization is found to be in the microsecond range and is fast enough to influence some ion transport systems. Nonlinearities in the force dependence of the membrane reorganization indicate that large responses could persist even at significantly lower field strengths. It is also seen that critical demixing effects provide a mechanism for electric fields to induce separation between neutral molecules. Most notably, a significant enhancement or depletion of cholesterol around a charged object in the membrane is predicted for membranes near a miscibility critical point. This effect suggests an electrostatic mechanism which could participate in the sorting of proteins into cholesterol-rich domains in the membrane.

Although the system examined here offers only a generic example, the thermodynamic model and the methods of calculation are sufficiently general to accommodate nearly any field distribution and membrane composition. Continuum thermodynamic calculations such as the ones described here provide relatively efficient means of estimating dynamical processes in fluid membranes. It is our hope that simple calculations of this sort will help to make quantitative correlations between experimental measurements in systems such as supported bilayer membranes and lipid monolayers with actual processes occurring in the membranes of living cells.

Acknowledgment. We thank Professor Sunney Chan and the Institute of Chemistry, Academia Sinica in Taipei Taiwan for sponsoring J.T.G. while much of this work was completed (NSC 88-2113-M-001-037). We also thank Steven Andrews for assistance with the C programming and Professor Stuart McLaughlin for helpful comments on the manuscript. Additional funding was provided by NSF Biophysics Program grants to S.G.B. and H.M.M.

References and Notes

(1) Knowles, D. W.; Tilley, L.; Mohandas, N.; Chasis, J. A. *Proc. Natl. Acad. Sci. U.S.A.* **1997**, *94*, 12969−12974.
(2) Döbereiner, H.-G.; Käs, J.; Noppl, D.; Sprenger, I.; Sackmann, E. *Biophys. J.* **1996**, *71*, 648−656.
(3) Seifert, U. *Phys. Rev. Lett.* **1993**, *70*, 1335−1338.
(4) Chen, C.-M.; Higgs, P. G.; MacKintosh, F. C. *Phys. Rev. Lett.* **1997**, *79*, 1579−1582.
(5) Sackmann, E. *FEBS Lett.* **1994**, *346*, 3−16.
(6) McLaughlin, S.; Poo, M.-M. *Biophys. J.* **1981**, *34*, 85−93.
(7) Kloboucek, A.; Behrisch, A.; Faix, J.; Sackmann, E. *Biophys. J.* **1999**, *77*, 2311−2328.
(8) Nardi, J.; Bruinsma, R.; Sackmann, E. *Phys. Rev. E* **1998**, *58*, 6340−6354.
(9) Poo, M.-M.; Robinson, K. R. *Nature* **1977**, *265*, 602−605.

(10) Jaffe, L. F. *Nature* **1977**, *265*, 600−602.
(11) Ryan, T. A.; Myers, J.; Holowka, D.; Baird, B.; Webb, W. W. *Science* **1988**, *239*, 61−64.
(12) Groves, J. T.; Boxer, S. G.; McConnell, H. M. *Proc. Natl. Acad. Sci. U.S.A.* **1997**, *94*, 13390−13395.
(13) Grakoui, A.; Bromley, S. K.; Sumen, C.; Davis, M. M.; Shaw, A. S.; Allen, P. M.; Dustin, M. L. *Science* **1999**, *285*, 221−227.
(14) Kurzchalia, T. V.; Parton, R. G. *Curr. Opin. Cell Biol.* **1999**, *11*, 424−431.
(15) Simmons, K.; Ikonen, E. *Nature* **1997**, *387*, 569−572.
(16) Sheets, E. D.; Holowka, D.; Baird, B. *Curr. Opin. Chem. Biol.* **1999**, *3*, 95−99.
(17) Viola, A.; Schroeder, S.; Sakakibara, Y.; Lanzavecchia, A. *Science* **1999**, *283*, 680−682.
(18) Mouritsen, O. G.; Kinnunen, P. J. K. Role of lipid organization and dynamics for membrane functionality. In *Biological membranes. A molecular perspective from computation to experiment*; Merz, K. M., Roux, B., Eds.; Birkhäuser: Boston, 1996; pp 463−502.
(19) Harder, T.; Simons, K. *Curr. Opin. Cell Biol.* **1997**, *9*, 534−542.
(20) Gil, T.; Ipsen, J. H.; Mouritsen, O. G.; Sabra, M. C.; Sperotto, M. M.; Zuckermann, M. J. *Biochim. Biophys. Acta* **1998**, *1376*, 245−266.
(21) Marcelja, S. *Biochim. Biophys. Acta* **1976**, *455*, 1−7.
(22) Owicki, J. C.; McConnell, H. M. *Proc. Natl. Acad. Sci. U.S.A.* **1979**, *76*, 4750−4754.
(23) Pearson, T. L.; Edelman, J.; Chan, S. I. *Biophys. J.* **1984**, *45*, 863−871.
(24) Groves, J. T.; Boxer, S. G.; McConnell, H. M. *Proc. Natl. Acad. Sci. U.S.A.* **1998**, *95*, 935−938.
(25) Lee, K. Y. C.; Klingler, J. F.; McConnell, H. M. *Science* **1994**, *263*, 655−658.
(26) Keller, S. L.; Pritcher, W. H.; Heustis, W. H.; McConnell, H. M. *Phys. Rev. Lett.* **1998**, *81*, 5019−5022.
(27) Groves, J. T.; Boxer, S. G. *Biophys. J.* **1995**, *69*, 1972−1975.
(28) Stelzle, M.; Miehlich, R.; Sackmann, E. *Biophys. J.* **1992**, *63*, 1346−1354.
(29) Gennis, R. B. *Biomembranes*; Springer-Verlag: New York, 1989.
(30) Tu, K.; Klein, M. L.; Tobias, D. J. *Biophys. J.* **1998**, *75*, 2147−2156.
(31) Robinson, A. J.; Richards, W. G.; Thomas, P. J.; Hann, M. M. *Biophys. J.* **1995**, *68*, 164−170.
(32) Groves, J. T.; Boxer, S. G.; McConnell, H. M. *J. Phys. Chem. B* **2000**, *104*, 119−124.
(33) Bradshaw, R. W.; Robertson, C. R. *J. Membr. Biol.* **1975**, *25*, 93.
(34) Harvey, S. C. *Proteins* **1989**, *5*, 78−92.
(35) Steffen, M. A.; Lao, K.; Boxer, S. G. *Science* **1994**, *64*, 810−816.
(36) Doyle, D. A.; Cabral, J. M.; Pfuetzner, R. A.; Kuo, A.; Gulbis, J. M.; Cohen, S. L.; Chait, B. T.; MacKinnon, R. *Science* **1998**, *280*, 69−77.
(37) Radhakrishnan, A.; McConnell, H. M. *J. Am. Chem. Soc.* **1999**, *121*, 486-487.
(38) Radhakrishnan, A.; McConnell, H. M. *Biophys. J.* **1999**, *77*, 1507−1517.
(39) Jordan, P. C. Interactions of ions with membrane proteins. In *Thermodynamics of membrane receptors and channels*; Jackson, M. B., Ed.; CRC Press: Ann Arbor, MI, 1993.
(40) *Structure and Dynamics of Membranes*; Lipowsky, R., Sackmann, E., Eds.; Elsevier Science Ltd.: New York, 1995; Vol. 1.
(41) Hille, B. *Ion channels of excitable membranes*, 2nd ed.; Sinauer Associates: Sunderland, MA, 1992.